Electron Spin Adjustment in Manganocenes. Preparative, Paramagnetic NMR, and X-ray Study on Substituent and Solvent Effects[1]

Nikolaus Hebendanz, Frank H. Köhler,* Gerhard Müller, and Jürgen Riede

Contribution from the Anorganisch-Chemisches Institut, Technische Universität München, D-8046 Garching, West Germany. *Received August 5, 1985*

Abstract: The new manganocenes $(EtCp)_2Mn$ (**3**), $(Me_3SiCp)_2Mn$ (**6**), $(Me_2Cp)_2Mn$ (**7**), $(Me_4Cp)_2Mn$ (**8**), and $(EtMe_4Cp)_2Mn$ (**10**) have been prepared together with Cp_2Mn (**1**), $(MeCp)_2Mn$ (**2**), $(i\text{-}PrCp)_2Mn$ (**4**), $(t\text{-}BuCp)_2Mn$ (**5**), and $(Me_5Cp)_2Mn$ (**9**). Their ^1H, ^{13}C, and ^{29}Si NMR signals experience shifts up to 1340 ppm at 390 K and provide a systematology of shifts which allows a fast and detailed characterization. Low-spin ($^2E_{2g}$) and high-spin ($^6A_{1g}$) manganocenes are recognized easily, even in a mixture, due to very different shift ranges. These ranges and further particularities are explained in terms of different electron spin delocalization. The spin state of manganocenes depends on the *nature* of substituents R, the number of R, the solvent, and the temperature. $^2E_{2g}$ is favored by donor substituents and $^6A_{1g}$ by acceptors. $^2E_{2g}$ is also favored by increasing the *number* of donors: for $(RCp)_2Mn$ $^2E_{2g}$ and $^6A_{1g}$ species are found to be in equilibrium with 13% $^2E_{2g}$ for **2** (ΔH° = 11.6 kJ mol^{-1}, ΔS° = 44.5 J mol^{-1} K^{-1}), 30% for **7**, and no detectable $^6A_{1g}$ population for **8–10**, all at 400 K. The mixtures of $^2E_{2g}$ and $^6A_{1g}$ manganocenes in toluene are transformed to pure high-spin species when donor solvents are used. At low temperatures the NMR spectra of both manganocene spin isomers are observed in toluene. Coalescence is found for **2–6** near room temperature with a lifetime of 9.8×10^{-6} s for the spin isomers of **2** and $\Delta G^\ddagger$ = 49 kJ mol^{-1} for $^2E_{2g} \rightarrow {}^6A_{1g}$. $(Me_3SiCp)_2Mn$ turns out to be the first pure high-spin manganocene at ambient temperature. The X-ray analysis of **6** at −35 °C shows discrete centrosymmetric monomers ($P2_1/n$, a = 6.362 (2) Å, b = 11.725 (3) Å, c = 12.628 (3) Å, β = 94.48 (2)°, V = 939.10 Å^3, d_{calcd} = 1.166 g/cm^3 for Z = 2, R_w = 0.040 for 104 parameters and 1379 observables). The crystal packing is largely determined by the silyl groups, and unlike in Cp_2Mn no bridging ligands are present. The distance Mn–Cp(centroid) is 2.050 (3) Å. The rings are slightly slipped such that the silyl bearing carbons form the shortest bonds to Mn. This is explained by MO arguments.

In the metallocene series the best candidate to accomplish important property changes by simply modifying the cyclopentadienyls most probably is manganocene. Cp_2Mn has five unpaired electrons near room temperature with some antiferromagnetic coupling[2] and its Cp–metal bond is considerably ionic as compared to other metallocenes. This is reflected in an unusually long metal–ligand distance as determined in the gas phase,[3] in facile Cp exchange,[2d,4] and in the fact that conducting solutions in THF are obtained.[2d] In contrast, decamethylmanganocene $(Me_5Cp)_2Mn$ has only one unpaired electron;[5] the Cp–metal bond is much shorter,[6] and no ligand exchange can be detected.[5a] This is consistent with a rather covalent bonding.

While $(Me_5Cp)_2Mn$ is exclusively low-spin $^2E_{2g}$ up to 313 K,[5a,b] no manganocene seems to have been obtained which is a pure high-spin $^6A_{1g}$ species at room temperature regardless whether it be in solution or in the solid state. Actually, a low-spin–high-spin equilibrium exists over a wide temperature range. This has been shown for manganocene and 1,1′-dimethylmanganocene, $(MeCp)_2Mn$, by photoelectron spectroscopy,[7] by magnetic measurements in solution,[8] by ESR spectroscopy,[8,9] and by electron diffraction.[10] For 1,1′-di-*tert*-butylmanganocene, $(t\text{-}BuCp)_2Mn$, the equilibrium has been followed by magnetic measurements and optical spectroscopy; no details were given on the preparation of the compound.[11]

The spin equilibrium may also be observed in the ^1H NMR spectrum of 1,1′-diisopropylmanganocene, $(i\text{-}PrCp)_2Mn$, as we mentioned briefly.[12] Before work in this laboratory was started,[1] no systematic NMR investigation of manganocenes appeared. Nevertheless, an impetus was given as early as 1958 when McConnell and Holm reported a proton signal for Cp_2Mn.[13] It appears high field relative to a standard while Switzer et al. note a low field shift.[8] The latter authors also give ^1H data for $(MeCp)_2Mn$ which are at variance with our results for $(i\text{-}PrCp)_2Mn$.[12] Therefore, we wished to obtain a reliable NMR basis from a more thorough investigation of manganocenes as the missing link in our NMR studies of paramagnetic metallocenes.[14]

The reactivity of manganocenes depends markedly on their spin state; e.g., $(Me_5Cp)_2Mn$ gives an isolable cation and anion while Cp_2Mn does not.[5a,b] We have observed that $(MeCp)_2Mn$ comproportionates with manganese dihalides in the presence of a donor to give half-sandwiches of the type $[(MeCp)MnX(PEt_3)]_2$.[15] But

(1) Extracted from the Diplomarbeit and Dissertation of N. H. (Technische Universität München 1981 and 1984). Presented in part at the Chemiedozententagung, Kaiserslautern, 1982.

(2) (a) Fischer, E. O.; Leipfinger, H. *Z. Naturforsch., B: Anorg. Chem., Org. Chem. Biochem., Biophys., Biol.* **1955**, *10*, 353–355. (b) Leipfinger, H. *Ibid.* **1958**, *13*, 53–54. (c) Voitländer, J.; Schimitschek, E. *Z. Elektrochem.* **1957**, *61*, 941–943. (d) Wilkinson, G.; Cotton, F. A.; Birmingham, J. M. *J. Inorg. Nucl. Chem.* **1956**, *2*, 95–113. (e) Krieger, R.; Voitländer, J. *Z. Naturforsch., A: Phys., Phys. Chem., Kosmophys.* **1972**, *27*, 1082–1092. (f) König, E.; Desai, V. P.; Kanellakopulos, B.; Klenze, R. *Chem. Phys.* **1980**, *54*, 109–113.

(3) (a) Almenningen, A.; Haaland, A.; Motzfeld, T. *Selected Topics in Structure Chemistry*; Universitetsforlaget: Oslo, 1967; p 105. (b) Haaland, A. *Top. Curr. Chem.* **1975**, *53*, 1–23. (c) Haaland, A. *Inorg. Nucl. Chem. Lett.* **1979**, *15*, 267–269.

(4) Switzer, M. E.; Rettig, M. F. *J. Chem. Soc., Chem. Commun.* **1972**, 687–688.

(5) (a) Smart, J. C.; Robbins, J. L. *J. Am. Chem. Soc.* **1978**, *100*, 3936–3937. (b) Robbins, J. L.; Edelstein, N. M.; Cooper, S. R.; Smart, J. C. *Ibid.* **1979**, *101*, 3853–3857. (c) Robbins, J. L.; Edelstein, N.; Spencer, B.; Smat, J. C. *Ibid.* **1982**, *104*, 1882–1893.

(6) (a) Freyberg, D. P.; Robbins, J. L.; Raymond, K. N.; Smart, J. C. *J. Am. Chem. Soc.* **1979**, *101*, 892–897. (b) Fernholt, L.; Haaland, A.; Seip, R.; Robbins, J. L.; Smart, J. C. *J. Organomet. Chem.* **1980**, *194*, 351–355.

(7) (a) Rabalais, J. W.; Werme, L. O.; Bergmark, L.; Karlsson, L.; Hussain, M.; Siegbahn, K. *J. Chem. Phys.* **1972**, *57*, 1185–1192. (b) Evans, S.; Green, M. L. H.; Jewitt, B.; King, G. H.; Orchard, A. F. *J. Chem. Soc., Faraday Trans. 2*, **1974**, 356–376. (c) Cauletti, C.; Green, J. C.; Kelly, M. R.; Powell, P.; van Tilborg, J.; Robbins, J.; Smart, J. *J. Electron Spectrosc. Relat. Phenom.* **1980**, *19*, 327–357.

(8) Switzer, M. E.; Wang, R.; Rettig, M. F.; Maki, A. H. *J. Am. Chem. Soc.* **1974**, *96*, 7669–7674.

(9) (a) Ammeter, J. H.; Bucher, R.; Oswald, N. *J. Am. Chem. Soc.* **1974**, *96*, 7833–7835. (b) Ammeter, J. H. *J. Magn. Reson.* **1978**, *30*, 299–325.

(10) Almenningen, A.; Haaland, A.; Samdal, S. *J. Organomet. Chem.* **1978**, *149*, 219–229.

(11) Ammeter, H.; Zoller, L.; Bachmann, J.; Baltzer, P.; Gamp, E.; Bucher, R.; Deiss, E. *Helv. Chim. Acta* **1981**, *64*, 1063–1082.

(12) Köhler, F. H.; Hebendanz, N. *Chem. Ber.* **1983**, *116*, 1261–1263.

(13) McConnell, H. M.; Holm, C. H. *J. Chem. Phys.* **1958**, *28*, 749–750.

(14) Köhler, F. H.; Geike, W. *J. Organomet. Chem.* **1983**, *256*, C27–C29 and preceeding papers in this series.

0002-7863/86/1508-3281$01.50/0 © 1986 American Chemical Society

Table I. Paramagnetic ^1H, ^{13}C, and ^{29}Si Shifts (δ^{para}) at 390 K for Manganocenes Dissolved in Toluene-d_8 or as Neat Liquids

compd	nucleus	hydrogen or carbon position[a] 1	2/5	3/4	α	β	δ(^{29}Si)
Cp_2Mn	^1H	−23.3	−23.3	−23.3			
	^{13}C	−1206	−1206	−1206			
$(Mecp)_2Mn$	^1H		−8.1	−73.7	−129.0		
	^{13}C	−1340	−846	−1116	130.9		
$(EtCp)_2Mn$	^1H		−12.6	−59.9	−110.7	−9.0	
	^{13}C	−1263	−929	−1094	141.5	−498.3	
$(i\text{-}PrCp)_2Mn$	^1H		−16.7	−49.4	−93.4	−10.6	
	^{13}C	−1210	−969	−1078	148.4	−408.3	
$(t\text{-}BuCp)_2Mn$	^1H		−14.2	−41.7		−8.8	
	^{13}C	−1249	−1019	−1098	165.2	−351.4	
$(Me_3SiCp)_2Mn$	^1H		−40.9	30.6		−9.9	
	^{13}C	−912	−1388	−1196		−219.2	−231.0
$(Me_2Cp)_2Mn$	^1H	−12.8	−9.9		−44.9		
	^{13}C	−563	−200	−317	106.6		

[a] Numbering according to Figures 1–3. For $(Me_2Cp)_2Mn$ the numbering is symmetry adapted with carbon one lying on the C_2 axis of the isolated ligand.

we were unable to isolate a similar compound from peralkylated manganocenes.

The various differences led us to explore the limits of a spin state adjustment for manganese sandwiches. This report deals with the synthesis of a series of manganocenes where one substituent per Cp varies as well as the number of alkyls per Cp. We present a complete set of paramagnetic NMR data together with its use for the understanding of these molecules and the crystal structure of a high-spin manganocene which has the expected pentahapto bonding contrary to what is known from Bünder and Weiss' work on Cp_2Mn.[16]

Results

Syntheses. Anhydrous manganese dihalides, preferably the readily available $MnCl_2$,[17] are useful starting materials for the synthesis of substituted manganocenes. In THF the reaction with cyclopentadienide is promoted by the intermediate exothermic formation of a solvate complex (isolable as $MnCl_2 \times 1.5$ THF[18]) which is moderately soluble. While sodium cyclopentadienides are sufficient for the preparation of Cp_2Mn, **1**,[2d] and $(MeCp)_2Mn$, **2**,[19] the average overall yields are better when substituted cyclopentadienes are transformed to the potassium salts with potassium hydride and then reacted with manganese dihalide. This is due to the superior metalating power of KH and the better solubility of RCpK in THF. $(EtCp)_2Mn$ (**3**), $(i\text{-}PrCp)_2Mn$ (**4**), $(Me_3SiCp)_2Mn$ (**6**), and $(1,2\text{-}Me_2Cp)_2Mn$ (**7**) may be obtained in yields up to 80%. The reaction time can be decreased by substituting a higher boiling ether for THF; e.g., dimethoxyethane is advantagous for the preparation of $(t\text{-}BuCp)_2Mn$, **5**.

The manganocenes **2**–**7** are liquids at room temperature or slightly above. Thus distillation is an efficient purification method. We use a specially designed apparatus[20] with a very slow product stream so that ubiquitous organic byproducts may be separated at the beginning and 10-g quantities of analytically (often even NMR spectroscopically) pure manganocene may be obtained.

Lithium cyclopentadienides are preferred starting materials when higher alkylated manganocenes are to be made. For $(Me_4Cp)_2Mn$ (**8**) and $(EtMe_4Cp)_2Mn$ (**10**) we use a procedure similar to our earlier work[21,22] except that **10** gives a better yield after sublimation rather than crystallization. Following Robbins' work[5c] we find, that $(Me_5Cp)_2Mn$ (**9**) is analytically pure already after sublimation.

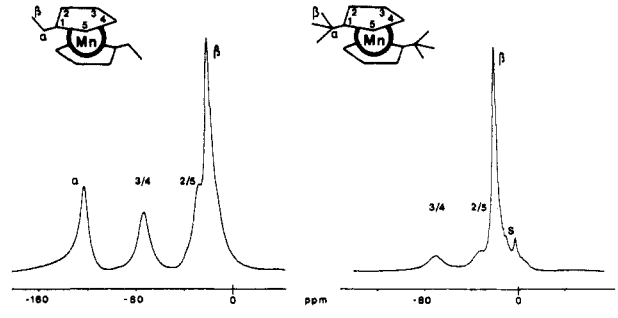

Figure 1. ^1H NMR spectra of pure $(EtCp)_2Mn$ and $(t\text{-}BuCp)_2Mn$ in toluene-d_8 at 390 K. S = solvent. The shift is linked arbitrarily to Me_4Si as zero since experimental spectra do not give uniform paramagnetic shifts (see also Figures 2–4).

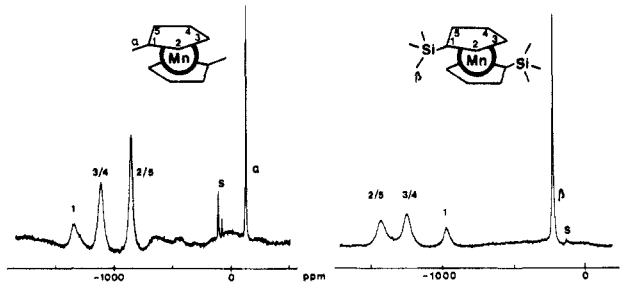

Figure 2. ^{13}C NMR spectra of molten $(MeCp)_2Mn$ and $(Me_3SiCp)_2Mn$ at 390 K. S = traces of naphthalene added as internal standard.

^1H, ^{13}C, and ^{29}Si NMR Spectra. Near room temperature the monosubstituted manganocenes **2**–**5** give ^1H NMR spectra which are difficult to interpret because unusually large line widths lead to signal overlap and integration problems. For ^{13}C the result is worse; no five-membered ring carbons may be observed even when pure liquid compounds are studied. After heating, better spectra are obtained; examples are given in Figures 1 and 2. They illustrate the signal assignment which is based on the change of substituents: on going from **3** to **5** the Hα signal disappears, we still have Hβ while H2–5 remain essentially unchanged. Similarly, in Figure 2 C1, C2–5, Cα, and Cβ are recognized. This is supported by the signal areas, although especially in ^1H NMR the integrations alone may be insufficient for the assignment. The paramagnetic shifts at 390 K, δ_{390}^{para} are collected in Table I. It is interesting to note that small quantities of naphthalene used

(15) Köhler, F. H.; Hebendanz, N.; Thewalt, U.; Kanellakopulos, B.; Klenze, R. *Angew. Chem.* **1984**, *96*, 697–699; *Angew. Chem., Int. Ed. Engl.* **1984**, *23*, 721–722.
(16) Bünder, W.; Weiss, E. *Z. Naturforsch., B: Anorg. Chem. Org. Chem.* **1978**, *33*, 1235–1237.
(17) Brauer, G. *Handbuch der Präparativen Anorganischen Chemie*; Enke: Stuttgart, 1981; Vol. III, p 1842.
(18) Kern, R. J. *J. Inorg. Nucl. Chem.* **1962**, *24*, 1105–1109.
(19) Reynolds, L. T.; Wilkinson, G. *J. Inorg. Nucl. Chem.* **1959**, *9*, 86–92.
(20) Köhler, F. H.; Prössdorf, W. *Z. Naturforsch., B: Anorg. Chem. Org. Chem.* **1977**, *32*, 1026–1029.
(21) Köhler, F. H.; Doll, K. H. *Z. Naturforsch., B: Anorg. Chem. Org. Chem.* **1982**, *37*, 144–150.
(22) Köhler, F. H.; Doll, K. H.; Prössdorf, W. *J. Organomet. Chem.* **1982**, *224*, 341–353 and cited literature.

Table II. Paramagnetic ^1H and ^{13}C Shifts (δ^{para}) for Low-Spin Manganocenes Dissolved in Toluene-d_8

			hydrogen or carbon position[a]							
compd	temp (K)	nucleus	1	2/5	3/4	α1	α2/5	and	α3/4	β
$(MeCp)_2Mn$	196	^1H		7.8	4.2	−39.6				
	200	^{13}C	−250.3	61.9	−49.5	160.5				
$(EtCp)_2Mn$	196	^1H		14.9	10.9	−23.7				16.0
	215	^{13}C	−188.9	35.0	−43.5	137.2				−45.9
$(i\text{-}PrCp)_2Mn$	196	^1H		6.1	6.1	−14.4				12.2
	215	^{13}C	−172.8	28.2	−44.6	128.3				−30.2
$(t\text{-}BuCp)_2Mn$	196	^1H		6.2	6.2					11.9
	225	^{13}C	−151.1	32.4	−37.9	116.9				−13.0
$(Me_2Cp)_2Mn$	196	^1H	7.0[a]	1.9[a]				−36.0[a]		
	215	^{13}C	131.1[a]	83.1[a,b]	−166.6[a,b]			158.7[a]		
$(Me_4Cp)_2Mn$	298[c]	^1H	5.5[a]				6.5[a]		−5.6[a]	
	298[c]	^{13}C	25.5[a]	−52.7[a]	−2.7[a]		131.9[a]		133.8[a]	
$(Me_5Cp)_2Mn$	298[c]	^1H				5.1	5.1		5.1	
	298[c]	^{13}C	−10.6	−10.6	−10.6	150.4	150.4		150.4	
$(EtMe_4Cp)_2Mn$	298[c]	^1H				13.4	2.4		5.4	−5.2
	298[c]	^{13}C	17.3	7.7[b]	23.1[b]	141.5	148.5		148.5	63.6

[a] Numbering according to Figures 1–3. For $(Me_2Cp)_2Mn$ and $(Me_4Cp)_2Mn$ the numbering is symmetry adapted with carbon one lying on the C_2 axis of the isolated ligand. [b] Assignment unclear. [c] Converted from varying experimental temperatures which were up to 9 °C higher; the deviation from the Curie law is very small as verified experimentally.

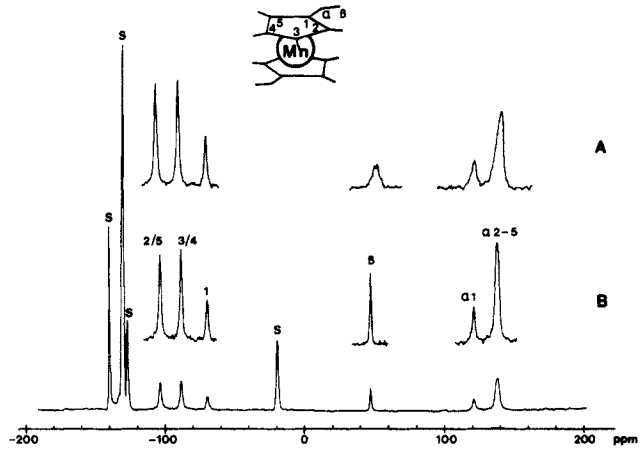

Figure 3. ^{13}C NMR spectrum of $(EtMe_4Cp)_2Mn$ in toluene-d_8 at 305 K. S = solvent. Trace A: ^{13}C. B and lowest trace: $^{13}C\{^1H\}$.

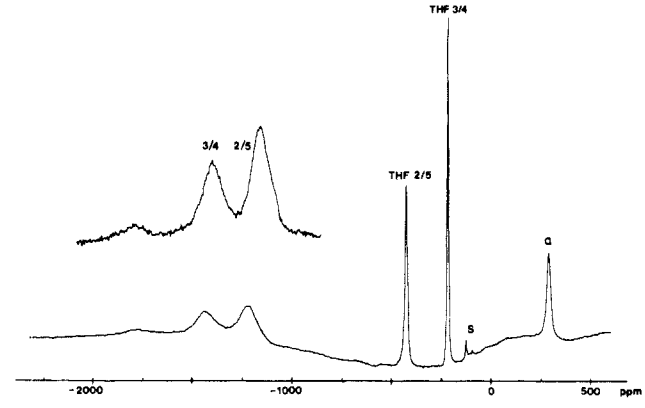

Figure 4. ^{13}C NMR spectrum of $(MeCp)_2Mn$ in THF at 303 K. S = traces of naphthalene added as internal standard.

as a secondary reference in pure liquid manganocenes at high temperature has inverted ^{13}C signals (cf. Figures 2 and 4). The quaternary carbons appear high field from the tertiary ones (e.g., 34 ppm in the spectrum of **2**, Figure 2) contrary to what is well-known from usual samples. As we have shown earlier[23] this effect is due to a preferred orientation of a metallocene relative to other anisotropic molecules like naphthalene. It decreases with increasing temperature as well as on dilution, it is much less important for aromatic carbons bearing a proton, and it is almost negligible for paramagnetic proton NMR. Accordingly we have minimized the error introduced into the $\delta^{para}(^{13}C)$.

Completely different spectra are obtained for the polyalkylated manganocenes **8–10**; an example is given in Figure 3. The signal assignment is again assured by the variation of the substituents and by signal intensities. The ^{13}C signals are so narrow that $^1J(CH)$ multiplets or signal broadening due to residual coupling may be observed (cf. Figure 3), and decoupling establishes the surprising fact that the Cα signals are more shifted than those of C1–5.

At low temperature both types of spectra, with broad signals and large shifts as in Figures 1 and 2 or with narrow signals and smaller shifts as in Figure 3, may be observed in the ^1H NMR for all monosubstituted manganocenes except **6**. As will be discussed in detail later they originate from the high-spin and low-spin isomer of each manganocene. An example is the ^1H spectrum of **2** at 223 K in Figure 5. Manganocenes **3–5** are less favorable cases because the Hβ of both spin isomers, two five-membered ring protons of the high-spin isomer and H2–5 as well as Hα of the low-spin isomer appear in a range of ca. 20 ppm. They tend to bury the reference signals, and they overlap severely so that at present we can extract the ^1H data for **3–5** only below 200 K. A much better separation of low- and high-spin signals is met in the ^{13}C NMR. Due to the low concentration and the enormous line widths for C1–5 of the high-spin isomer these signals are absent at low temperature. Thus, for **3–5** the analysis of the low-spin spectra is much easier in ^{13}C as compared to ^1H NMR. The data are summarized in Table II.

When high-spin manganocenes are dissolved in ethers instead of toluene, their signals are shifted largely and broad as well. An example is Cp_2Mn in THF-d_8 with $\delta_{335}^{para}(^{13}C)$ −1240. However, at comparable temperatures the shifts are somewhat smaller than in Table I, and a considerable displacement of the THF signals as shown in Figure 4 is observed. Similarly $(MeCp)_2Mn$ in 1,2-dimethoxyethane gives $\delta_{345}^{para}(^{13}C)$ −1370 (C1); −1090, −929 (C2–5); 376 (Cα); −268 (DME,CH_2); −54 (DME,CH_3).

Variable Temperature NMR. Combining the above findings in a variable temperature ^1H NMR study we find that the interconversion of manganocene spin isomers is a dynamic process which may lead to signal coalescence just near room temperature. A particularly good example is $(MeCp)_2Mn$, and selected spectra of a variable temperature series are shown in Figure 5. As a consequence of the high-spin–low-spin equilibrium the temperature dependence of the signal shifts is complex. The methyl resonance of **2** is most suitable for the analysis.

Temperature effects may be nicely followed by the reduced paramagnetic shifts $\vartheta = \delta_T^{para}T/298$ which are proportional to the hyperfine coupling constants. Depending on the electronic structure of the molecule ϑ is constant with T or slightly deviates from a parallel to the T-axis. As shown in Figure 6 the latter

(23) Köhler, F. H. *Z. Naturforsch., B: Anorg. Chem. Org. Chem.* **1980**, *35*, 187–194.

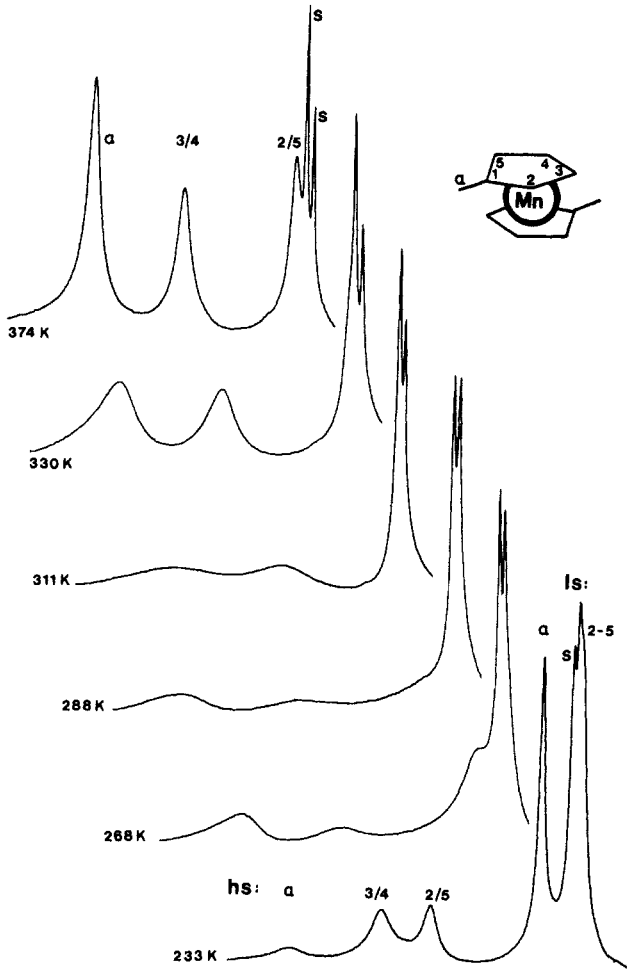

Figure 5. ^{1}H NMR spectra of $(MeCp)_2Mn$ in toluene-d_8, at selected temperatures. ls/hs = low-spin/high-spin isomer.

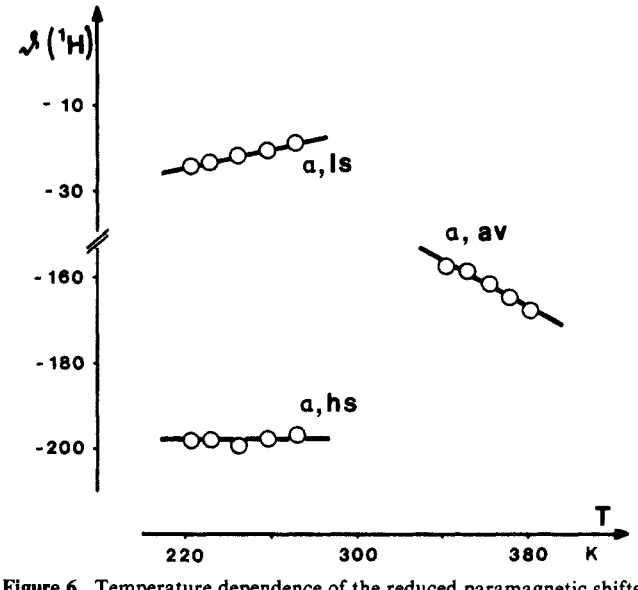

Figure 6. Temperature dependence of the reduced paramagnetic shifts for the methyl ^{1}H resonances of $(MeCp)_2Mn$: high-spin, $\delta(H\alpha,hs)$; low-spin, $\delta(H\alpha,ls)$; average, $\delta(H\alpha,av)$.

behavior is found below coalescence for low-spin $(MeCp)_2Mn$ with $\delta(H\alpha,ls)$ while $\delta(H\alpha,hs)$ is essentially constant. Above coalescence (cf. right part of Figure 6) $\vartheta(H\alpha,av)$ has contributions of both spin isomers; with increasing temperature it tends to the high-spin limiting shift. $\vartheta(H\alpha,ls)$ and $\vartheta(H\alpha,hs)$ at higher temperatures may be obtained via the ϑ-T curves (cf. Supplementary Material). Comparison of these shifts with the weighted average shift actually

Table III. Summary of Crystal Structure Data for $(Me_3SiCp)_2Mn$ (6)

formula	$C_{16}H_{26}MnSi_2$	scan type	ω
fw	329.496	scan width, deg	1.0
cryst syst	monoclinic	scan speed, deg/min	0.9 - 29.3
space group	$P2_1/n$	$(\sin\vartheta/\lambda)_{max}$, Å^{-1}	0.594
a, Å	6.362 (2)	hkl-range	+7, +13, ±14
b, Å	11.725 (3)	refl measd	1805
c, Å	12.628 (3)	refl unique	1651
β, deg	94.48 (2)	R_{int}[a]	0.041
V, Å^3	939.10	refl obsd	1379
Z	2	$[F_o > 4.0\sigma(F_o)]$	
d_{calcd}, g/cm^3	1.166	params ref	104
μ(Mo K_α)	7.88	R[b]	0.038
F(000), e	350	R_w[c]	0.040
T, °C	-35	$(\text{shift/error})_{max}$	0.63
radiatn	Mo Kα	$\Delta\rho_{fin}$(max/min), e/Å^3	0.32/-0.28
λ, Å	0.71069		

[a] $R_{int} = [\sum(N\sum_n w(\langle F\rangle - F)^2)/\sum((N-1)\sum_n wF^2)]^{1/2}$. [b] $R = \sum(||F_o| - |F_c||)/\sum|F_o|$. [c] $R_w = [\sum w(|F_o| - |F_c|)^2/\sum wF_o^2]^{1/2}$, $w = k/\sigma^2(F_o)$, $k = 1.9$.

Table IV. Fractional Atomic Coordinates and Equivalent Isotropic Thermal Parameters for the Non-H Atoms of $(Me_3SiCp)_2Mn$

atom	X/A	Y/B	Z/C	U(eq)[a]
Mn	0.5000 (0)	0.5000 (0)	0.5000 (0)	0.038
Si	0.7077 (1)	0.4701 (1)	0.2383 (1)	0.034
C1	0.6241 (4)	0.5688 (2)	0.3433 (2)	0.029
C2	0.4208 (5)	0.6177 (2)	0.3523 (2)	0.035
C3	0.4293 (5)	0.6930 (2)	0.4394 (2)	0.038
C4	0.6361 (6)	0.6920 (2)	0.4857 (2)	0.040
C5	0.7553 (5)	0.6167 (2)	0.4282 (2)	0.036
C11	0.9078 (5)	0.3684 (3)	0.2999 (2)	0.050
C12	0.8321 (6)	0.5528 (3)	0.1344 (3)	0.060
C13	0.4765 (6)	0.3902 (3)	0.1794 (3)	0.065

[a] $U_{eq} = (U_1U_2U_3)^{1/3}$, where U_i are the eigenvalues of the U_{ij} matrix.

measured leads to the relative concentration of the low- and high-spin isomer. We thus obtain the temperature dependence of the equilibrium ls-$(MeCp)_2Mn$ → hs-$(MeCp)_2Mn$, and standard procedures (cf. Supplementary Material) give the thermodynamic parameters $\Delta H° = 11.6$ kJ mol^{-1} and $\Delta S° = 44.5$ J mol^{-1} K^{-1}. Similar values are found for $(i\text{-PrCp})_2Mn$: $\Delta H° = 11.2$ kJ mol^{-1}, $\Delta S° = 41.6$ J mol^{-1} K^{-1}.

A coalescence temperature of 310 K is estimated from the maximum broadening of the ^{1}H NMR spectra of $(MeCp)_2Mn$. With $\Delta H°$ and $\Delta S°$ we calculate 70% high-spin and 30% low-spin isomer at coalescence which corresponds to a population difference $\Delta P = 0.4$. The activation energy, $\Delta G^‡$, of the spin transition and the lifetime, τ, of the spin isomers may be determined[24] with ΔP and the difference of the shifts at coalescence, $\delta_{310}^{para}(H\alpha) = \delta_{310}^{para}(H\alpha,ls) - \delta_{310}^{para}(H\alpha,hs)$. From the ϑ-T curves (cf. Figure 6) we obtain $\delta_{310}^{para}(H\alpha) = 35.20$ kHz, which leads to a barrier of $\Delta G^‡_{ls} = 49$ kJ mol^{-1} on going from low- to high-spin $(MeCp)_2Mn$ and backwards $\Delta G^‡_{hs} = 47$ kJ mol^{-1}, both at 310 K. The lifetime of the isomers at coalescence is $\tau = 9.8 \times 10^{-6}$ s.

Cp_2Mn shows a ^{1}H NMR signal which hardly moves with temperature. The ϑ-T behavior resembles that of $\vartheta(H\alpha,av)$ in Figure 6 suggesting a high-spin–low-spin equilibrium. However, no coalescence can be observed down to 180 K. Below 230 K the intensity of the signal decreases rapidly, and two new ones with roughly equal intensity and $\delta_{310}^{para}(^1H)$ −148 and 28.4 appear instead. Neither signal follows the Curie law; the deviation is similar to that found for antiferromagnetic molecules.[25]

$(Me_2Cp)_2Mn$ has much less shifted signals at 390 K than the $(RCp)_2Mn$ **2–5** (cf. Table I). It follows immediately that the additional alkyl per Cp reduces the population of the high-spin state. Accordingly, we are unable to detect high-spin isomers for the polyalkylated manganocenes **8–10** up to 400 K. On the

(24) Shanan-Atidi, H.; Bar-Eli, K. H. *J. Chem. Phys.* **1970**, *74*, 961–963.
(25) Köhler, F. H.; Cao, R.; Ackermann, K.; Sedlmair, J. *Z. Naturforsch., B: Anorg. Chem. Org. Chem.* **1983**, *38*, 1406–1411.

Table V. Principal Bond Lengths (Å) and Angles (deg) for $(Me_3SiCp)_2Mn$[a]

Mn–C1	2.331 (2)	C1–Si	1.867 (2)
Mn–C2	2.343 (3)	Si–C11	1.869 (3)
Mn–C3	2.420 (2)	Si–C12	1.858 (3)
Mn–C4	2.423 (3)	Si–C13	1.850 (4)
Mn–C5	2.359 (3)		
C1–C2	1.427 (4)		
C2–C3	1.409 (4)		
C3–C4	1.397 (5)		
C4–C5	1.402 (4)		
C5–C1	1.422 (4)		
C5–C1–C2	105.3 (2)	C1–Si–C11	108.8 (1)
C1–C2–C3	109.5 (3)	C1–Si–C12	109.8 (1)
C2–C3–C4	107.4 (3)	C1–Si–C13	109.8 (1)
C3–C4–C5	108.6 (3)	C11–Si–C12	108.2 (2)
C4–C5–C1	109.2 (3)	C11–Si–C13	109.8 (2)
C2–C1–Si	128.0 (2)	C12–Si–C13	110.4 (2)
C5–C1–Si	126.7 (2)		

[a] With esd's in units of the last significant figure in parentheses.

contrary, no low-spin isomer can be found for $(Me_3SiCp)_2Mn$, **6**, in ^1H NMR down to 215 K. The latter finding prompted us to perform X-ray studies on **6** since no solid-state structure of an unperturbed high-spin manganocene is known so far.

X-ray Structure of $(Me_3SiCp)_2Mn$. The solid-state structure of **6** at −35 °C shows discrete, monomeric molecules with crystallographically imposed centrosymmetry (Figure 7, Tables III–V). As a consequence, the Cp rings are parallel and in a staggered conformation with the Me_3Si substituents in trans positions. As is evident from the variation in Mn–C(Cp) bond lengths the (essentially planar) Cp rings are slightly asymmetrically bonded to Mn resulting in a small slippage of the top and bottom halves of the metallocene.

Hence the line joining Mn and the centroid of the Cp ring (see Figure 7a) and the normal to the ring are not coincident but form an angle of 3.2°. The difference in length between the former line and the distance of Mn from the ring is minimal however (2.050 (3) vs. 2.047 (3) Å, respectively). The Me_3Si group bonded at C1 is responsible for this effect. This is reflected in the bond lengths: M–C increases smoothly from 2.331 (2) Å for C1 to 2.420 (2)/2.423 (3) Å for C3/4; the C–C bonds of the ring which include C1 are slightly longer than the others. The fact that the silyl-bearing C atom comes *closest* to Mn points to an electronic effect while the steric bulk of the trimethylsilyl group is expected to favor an opposite trend (cf. Discussion below). The Me_3Si group is slightly bent out of the Cp plane *away* from the Mn atom as manifested by an angle of 2.9° between the C1–Si bond and the best plane through the ring atoms. This effect is minor, however, and does not result in a significant pyramidalization of C1.

Figure 7b gives a space-filling representation of **6**. From this it is immediately obvious that the bulky Me_3Si groups do not lead to severe steric interactions between the two Cp rings nor is the central high-spin manganese atom uniformly shielded by them. Although the ring hydrogens were refined, no definite conclusion can be drawn as to their relative orientation with respect to the C_5 ring. The relatively high standard deviations associated with these atoms render the observed small deviations from planarity insignificant.

Discussion

Three problems have obscured the NMR studies of manganocenes so far. (i) In the solid state the magnetic behavior is complicated by intermolecular interactions,[2] and NMR signals experience a bulk susceptibility shift to high field. This is why McConnell and Holm[13] find a high field ^1H signal for Cp_2Mn while in solution and with an internal standard we compensate these effects and obtain $\delta_{310}^{para}(^1H)$ −23.3 in accord with Switzer et al.[8] (paramagnetic low field shifts are negative). (ii) For many manganocenes the spin crossover leads to a coalescence of the ^1H NMR signals just near room temperature. The work of Switzer et al.[8] suffers from this problem; one signal has been overlooked, and hence the authors give an erroneous signal assignment. This

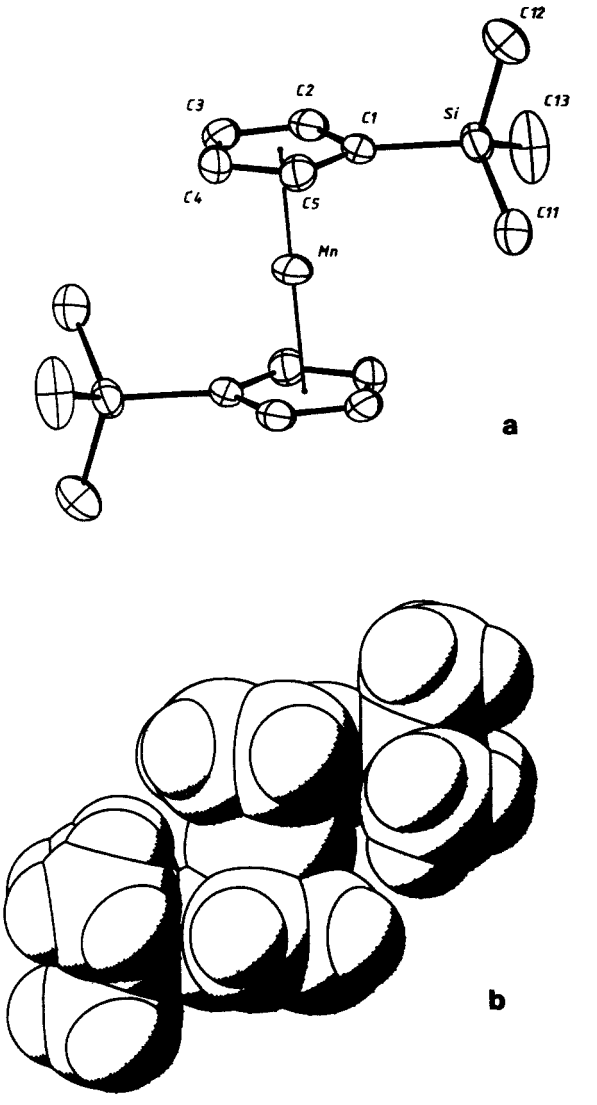

Figure 7. (a) ORTEP drawing of the molecular geometry of $(Me_3SiCp)_2Mn$ with atomic numbering scheme. (Thermal ellipsoids at the 50% probability level; H atoms omitted for clarity.) (b) Space-filling representation of **6** (PLUTO, the following "van der Waals" radii were used for the drawing: Mn, 1.9; Si, 1.8; C, 1.7; H, 1.2 Å).

in turn creates difficulties in the discussion of the spin delocalization. (iii) Due to the low receptivity of ^{13}C together with broad signals the signal-to-noise ratio may be bad. We have shown[12] that for manganocenes this problem can be overcome with high sample concentration, high temperature, and a high-power instrument.

Low-Spin–High-Spin Interconversion. Many properties of a manganocene can be studied within ca. 40 min, the recording time of the ^1H and ^{13}C spectrum. Besides the molecular structure it can be deduced whether the manganocene is low-spin or essentially high-spin. The spin delocalization (vide infra) leads to similar ^1H shift ranges for both spin isomers. High- and low-spin species may be distinguished easily by ^{13}C NMR with very different shift ranges (cf. Tables I and II). It should be emphasized, however, that in Table I pure high-spin data are given only for $(Me_3SiCp)_2Mn$ the others being averaged shifts.

Interestingly, the entropy and enthalpy term of the equilibrium $^2E_{2g}$-$(R_xCp)_2Mn \rightarrow {}^6A_{1g}$-$(R_xCp)_2Mn$ is rather similar for $(MeCp)_2Mn$ and $(i\text{-}PrCp)_2Mn$. Inspection of the ^1H NMR spectra of $(EtCp)_2Mn$ and $(t\text{-}BuCp)_2Mn$ yields $\Delta H^\circ \approx 11$–$13$ kJ mol^{-1} and $\Delta S^\circ \approx 40$–$50$ J mol^{-1} K^{-1} as well. This agrees with Ammeter's[11] data on $(t\text{-}BuCp)_2Mn$ whereas Switzer's[8] data on $(MeCp)_2Mn$ appear much too small. Accordingly, we find a 84% population of the high-spin isomer for $(MeCp)_2Mn$ at 100 °C which is distinctly higher than Haaland[10] obtained after fitting

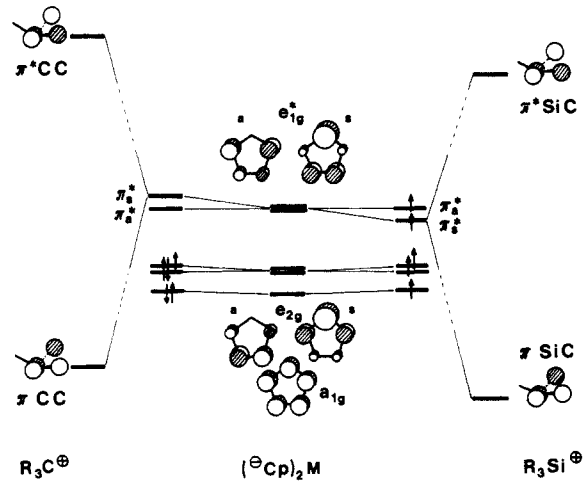

Figure 8. Perturbation of the metallocene frontier orbitals on replacing a hydrogen by alkyl or silyl substituents (cf. text). The electron count is given for M = Mn at low temperature.

the electron diffraction results of a high-spin–low-spin mixture of $(MeCp)_2Mn$.

There is a characteristic increase of the low-spin–high-spin ratio and the coalescence temperature with the number of alkyls attached to the cyclopentadienyl. For instance, an averaged signal is observed for Cp_2Mn down to 180 K, and the ^1H spectra of $(RCp)_2Mn$ collapse around 310 K. Similarly, at 400 K the high-spin isomer content is about 87% for $(MeCp)_2Mn$, it is much lower for $(Me_2Cp)_2Mn$, and no high-spin isomer is found for $(Me_4Cp)_2Mn$ as well as for $(R_5Cp)_2Mn$. The number of substituents per Cp is too simple an idea to account for these trends because $(Me_3SiCp)_2Mn$ is high-spin in the accessible temperature range while the $(RCp)_2Mn$ **2–5** are partly low-spin.

Better insight is provided by changes in the known frontier orbitals[26] of a metallocene. Figure 8 shows their Cp content and how it is perturbed by replacing one hydrogen for a substituent.[27] We only care for e_{1g}* while e_{2g} and a_{1g} are essentially metal orbitals. The C–R and Si–R bonds are taken as sets of π and π* orbitals; one of each is shown. According to the symmetry the degeneracy of the manganocene orbitals is lifted in a three orbital interaction: the net acceptor SiR_3 stabilizes the symmetric e_{1g}* orbital while CR_3 has the opposite effect. As a consequence, SiR_3 lowers the energy gap between e_{1g}* and e_{2g} or a_{1g} and favors the high-spin isomer. Inversely, CR_3 favors the low spin isomer as found in the experiments. The effect of various host lattices on the spin crossover point of Cp_2Mn[9b] is similar to the influence of the substituents discussed here. As a difference the substitution effect also works in solution.

On going from Cp_2Mn to $(R_5Cp)_2Mn$ increasing substitution raises the energy of the ligand π orbitals and leads to a better energy match (and overlap) especially of the ligand e_1'' orbitals and the corresponding metal orbitals. Hence, in $(Me_5Cp)_2Mn$ the e_{1g}* orbitals are destabilized as compared to Cp_2Mn, the energy gap between e_{1g}* and e_{2g} or a_{1g} increases,[28] and the low-spin isomer is found.

The spin state of manganocenes seems to be influenced by the solvent as well. Molecules which have both spin isomers present in inert solvents like toluene are transformed to pure high-spin species in the presence of donor molecules like ethers. However, these species are no longer classical sandwiches because their NMR signal shifts differ from what we find for pure high-spin manganocenes. The strong paramagnetic signal shifts observed for the ether carbons indicate that the solvent is coordinated to manganese. The NMR results are consistent with the following structures A–C on the reasonable assumption that fast fluctuation gives a mean signal for η^5-, η^3-, and η^1-Cp (cf. exchange in paramagnetic Cp_3V[14]).

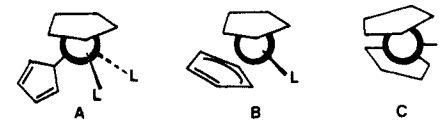

A is another example of the new half-sandwich type $CpMnXL_2$ we and others have established recently.[15,29] High-spin manganocene derivatives of type C are also known.[30] Finally, B and an equilibrium between A–C cannot be excluded at present.

Electron Spin Delocalization. The easy distinction of manganocene spin isomers by NMR is based on the different electron spin densities encountered at the ligand nuclei. It is, therefore, useful to know how the spin gets there. First we have to eliminate the electron nuclear coupling which does not proceed through bonds. For a preliminary estimate of the dipolar shifts, δ^{dip} we use McGarvey's equations;[31] a detailed analysis based on recent papers by Eicher[32] is in progress. Subtracting δ^{dip} from δ^{para} gives the contact shifts δ^{con} which are proportional to the spin densities in question. Since the g tensor of high-spin manganocenes can be taken to be isotropic,[9b] δ^{dip} vanishes. However, in Table I only the data for $(Me_3SiCp)_2Mn$ and $(Me_2Cp)_2Mn$ can be regarded as high-spin δ^{con} the others having some shift admixture from the low-spin isomer. For our qualitative discussion this will be neglected. From electron diffraction data[10,6b] and g values of samples in toluene glass[8,5b] we obtain $-5 < \delta_{298}{}^{dip}(^1H) < 10$ and $-150 < \delta_{298}{}^{dip}(^{13}C) < 10$. Details of the calculation of δ^{dip} are given in the Supplementary Material while the δ^{con} are reproduced in Figure 9.

The contact shift should increase with the number of unpaired electrons ($\delta^{con} \sim S(S+1)$).[33] This does not seem to be in accord with the ^1H data of the low- and high-spin manganocenes in Tables I and II. The inconsistency signals different delocalization to occur in both spin isomers for two reasons. (i) Even if an unpaired electron is in the same type of orbital for both isomers (e.g., e_{2g}-type), the ligand content in this orbital will be different due to different bond distances. (ii) The delocalization mechanism of an unpaired electron depends on the orbital type. We and others have shown[22] that in a metallocene e_{1g}* electrons experience direct π-delocalization while π-polarization and σ-delocalization work for a_{1g} and e_{2g} electrons. The π-mechanisms compensate more or less at each ligand nucleus. The effect of the remaining π-spin density adds to the σ-delocalization at the five-membered ring carbons, it subtracts at all nuclei next to these carbons, and it adds again after moving one bond further.

Combining these effects we see that in high-spin manganocenes with downfield shifts for C1–5 direct π-delocalization is the more efficient π-mechanism. This can be expected because π-polarization is a second order effect. $\delta^{para}(^1H\text{-ring})$ and $\delta^{para}(^{13}C\alpha)$ are small due to additional σ-delocalization which in turn enhances the downfield shift for C1–5, Hα, and Cβ. The latter two are shifted even further downfield due to hyperconjugational transfer of π-spin density from the five-membered ring carbons so that their signals have bigger shifts than those of H-ring and Cα. Clearly, the rule of thumb with a bigger shift for a nucleus closer to the spin source cannot hold in high-spin manganocenes. We have found for vanadocene halides[22] that whenever several delocalization mechanisms add to yield shifts near zero their sign can

(26) For a recent review, see: Clack, D. W.; Warren, K. D. *Struct. Bonding (Berlin)* **1980**, *39*, 1–41.
(27) For the interaction of doubly deprotonated manganocene and ER_3 in Figure 8 we neglect the formation of the σ-bond for simplicity.
(28) A similar reasoning has been presented by Smart[5c] in terms of the crystal field splitting.
(29) Heck, J.; Massa, W.; Weinig, P. *Angew. Chem.* **1984**, *96*, 699–700; *Angew. Chem., Int. Ed. Engl.* **1984**, *23*, 722–723.
(30) (a) Weed, J. T.; Rettig, M. F.; Wing, R. M. *J. Am. Chem. Soc.* **1983**, *105*, 6510–6511. (b) Howard, C. G.; Girolami, G. S.; Wilkonson, G.; Thornton-Pett, M.; Hursthouse, M. B. *Ibid.* **1984**, *106*, 2033–2040.
(31) Kurland, R. J.; McGarvey, B. R. *J. Magn. Reson.* **1970**, *2*, 286–301.
(32) (a) Eicher, H. *Chem. Phys.* **1984**, *86*, 331–338. (b) Eicher, H. *Ibid.* **1985**, *95*, 341–344.
(33) Jesson, J. P. In *NMR of Paramagnetic Molecules*; La Mar, G. N., Horrocks, W. DeW., Jr., Holm, R. H., Eds.; Academic Press: New York/London, 1973; pp 2–52.

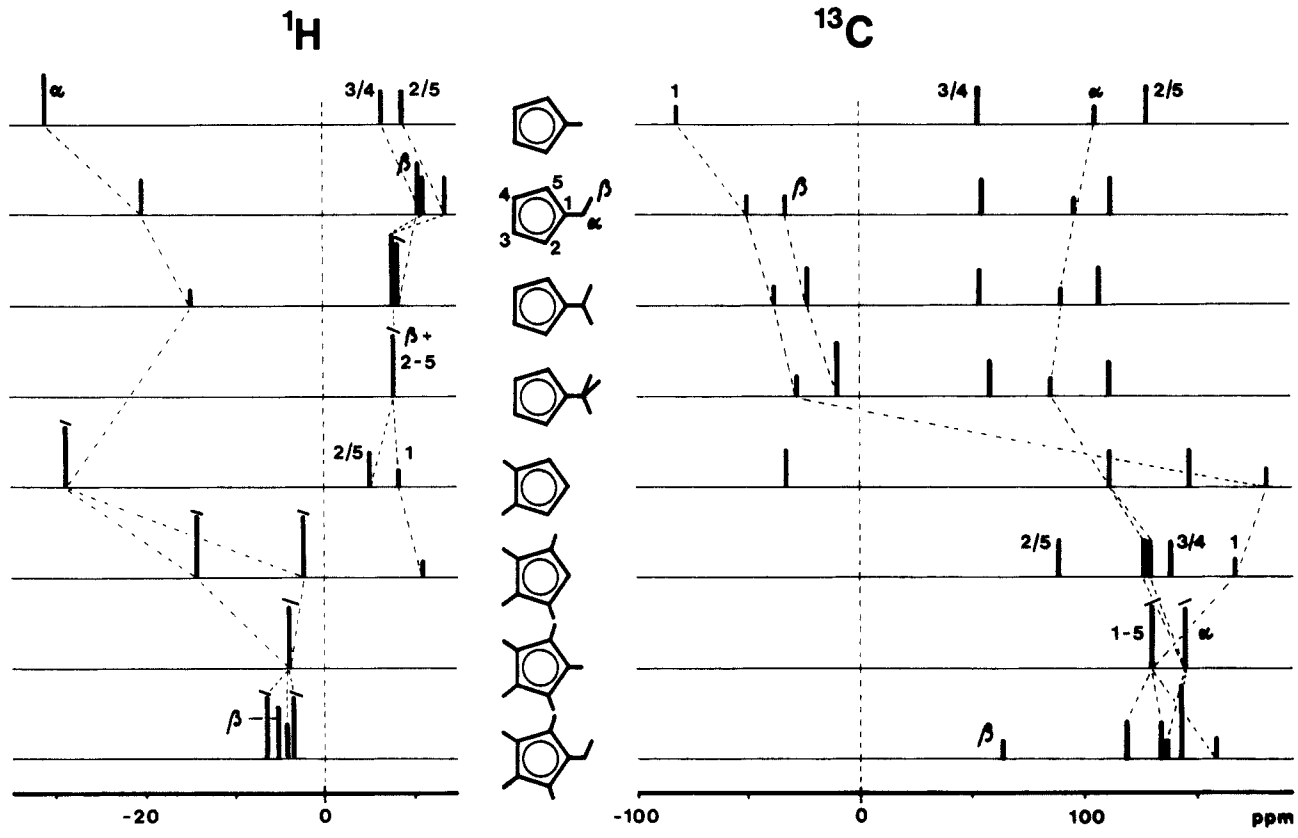

Figure 9. ^{1}H and ^{13}C contact shifts of low-spin manganocenes at 298 K. For comparison of the substitution pattern only one ligand is shown. The numbering is symmetry adapted as in Tables I and II.

be different for nuclei in corresponding positions. This is why $\delta^{para}(^{13}C\alpha)$ is small and positive while $\delta^{para}(^1H\text{-ring})$ is small and negative or positive (cf. $(Me_3SiCp)_2Mn$ and other $(RCp)_2Mn$ in Table I). A similar argument applies for $\delta_{310}{}^{para}(^{29}Si)$ −231,0; note that the ^{29}Si signal should be highfield like in $(Me_3SiCp)_2Co$ and $(Me_3SiCp)_2Ni$[34] if direct π-delocalization alone were present.

Our analysis is further supported by the signal splitting of the five-membered ring atoms. We note the striking fact that C1 is lowest field for the $(RCp)_2Mn$ **2–5** (cf. Table I and Figure 9), whereas it is highest field for $(Me_3SiCp)_2Mn$, $(Me_2Cp)_2Mn$, and $(Me_4Cp)_2Mn$. As in $(MeCp)_2M$ and $(Me_4Cp)_2M$ (M = V, Cr, Co, Ni)[21] the inversion is due to the lifting of the orbital degeneracy on substituting a metallocene. It may be opposite for different substitution patterns and/or substituents. We follow our earlier arguments[21,35] and assign signals of nuclei in positions 2/5 and 3/4 as given in Tables I and II or Figure 9. The distinction of α2/5 and α3/4 appears too speculative at present since these signals lie close together, and the procedure leading to δ^{con} is not very precise.

The small contact shifts for low-spin manganocenes may be understood in terms of the above mentioned antagonism of π-polarization and σ-delocalization. The presence of π-polarization follows from $\delta^{con}(^{13}C\beta)$ of $(EtCp)_2Mn$, **3**, and $(EtMe_4Cp)_2Mn$, **10**, because on going from **3** to **10** $\delta^{con}(^{13}C\beta)$ moves to high field (cf. Figure 9). Hyperconjugation is used here to probe the spin density in the Cp π-system (cf. details in ref 22). The presence of σ-delocalization is suggested by the fact that there is no sign inversion for δ^{con} on proceeding along some of the bonds. It must be emphasized, however, that a detailed comparison of the delocalization and the signal shifts is not yet satisfying. π-polarization and σ-delocalization can work simultaneously only when the unpaired electron resides in an e_{2g}-type orbital rather than

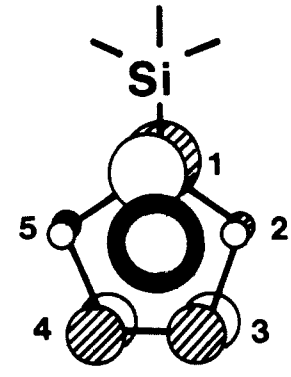

Figure 10. Silyl substitution and metal–carbon distances in η^5-cyclopentadienyl, cf. text.

a_{1g} since this allows the admixture of the lower lying σ-e_{2g}-type ligand orbital. Thus the NMR results provide another indication to an $^2E_{2g}$ ground state for low-spin manganocenes.

The Solid-State Structure of $(Me_3SiCp)_2Mn$. According to the NMR data $(Me_3SiCp)_2Mn$ should have a small if any admixture of a low-spin isomer. Actually, the X-ray analysis shows **6** to be the first isolated high-spin η^5-manganocene. As expected the 2.047 (3) Å Mn–Cp distance (defined as the distance of Mn from the least-squares plane for C1–5 or C1′–5′) is much longer than the 1.734 Å[6a] in crystalline $(Me_5Cp)_2Mn$, and it is identical with the distance found for high-spin Cp_2Mn in the gas phase.[3] There is hence an important intramolecular reorganization on going from low- to high-spin manganocene which is reflected in ΔH° of the equilibrium determined by NMR. Such a reorganization cannot usually be deduced from solution infrared data (except metal–ring vibration) which led Switzer et al.[8] to exclude major structural changes accompanying spin-state changes.

One interesting structural feature of $(Me_3SiCp)_2Mn$ is its unsymmetrical η^5-bonding. A ring slippage toward C1 occurs; Figure 10 gives an exaggerated view. While a similar distorsion in $^2E_{2g}$-$(Me_5Cp)_2Mn$ has been ascribed to the Jahn–Teller effect,[6a]

(34) Köhler, F. H.; Geike, W. *J. Magn. Reson.* **1983**, *53*, 297–302.
(35) A different population of two e-type orbitals as mentioned in ref 21 is not working in $^6A_{1g}$ manganocene since all frontier orbitals are singly occupied. Instead, the content of the original Cp e-orbitals in the manganocene orbitals becomes different after Cp substitution.

Table VI. Preparative and Analytical Data for Substituted Manganocenes

compd	$MnCl_2$,[a] g (mmol)	cyclopentadiene, g (mmol)	T,[b] °C	yield,[c] g (%)	mp, °C	anal. calcd (found)
$(EtCp)_2Mn$ (3)	4.50 (36)	6.86 (72.9)	D, 50–65	2.55 (29)	*f*	C: 69.71 (69.97); H: 7.52 (7.60); Mn: 22.77 (22.38)
$(i\text{-}PrCp)_2Mn$ (4)[d]	4.90 (39)	6.49 (60.0)	D, 70–78	5.30 (66)	*f*	C: 71.36 (71.15); H: 8.23 (8.22)
$t\text{-}BuCp)_2Mn$ (5)	4.61 (15)[e]	3.53 (28.9)	D, 110–120	3.55 (83)[g]	*f*	C: 72.71 (72.89); H: 8.81 (8.76); Mn: 18.48 (18.06)
$(Me_3SiCp)_2Mn$ (6)	6.25 (50)	12.74 (92.1)	D, 95–105	10.55 (70)	27–28	C: 58.32 (58.27); H: 7.95 (7.72); Mn: 16.67 (16.73); Si: 17.05 (17.9)
$(Me_2Cp)_2Mn$ (7)	3.25 (26)	5.53 (45.3)	D, 60–70	3.20 (69)	69–71	C: 69.71 (70.27); H: 7.52 (7.70)
$(Me_4Cp)_2Mn$ (8)	2.50 (20)	3.27 (26.8)	S, 90–95	2.45 (61)[h]	144–146	C: 72.71 (72.68); H: 8.81 (8.53)
$(EtMe_4Cp)_2Mn$ (10)	2.10 (17)	3.54 (23.6)	S, 90–95	2.75 (66)	100–101	C: 74.76 (74.58); H: 9.70 (9.48); Mn: 15.54 (15.27)

[a] Dissolved in THF. [b] Bath temperature for distillation (D) or sublimation (S). [c] Based on the cyclopentadiene. [d] We have prepared 3 also via *i*-PrCpNa.[14] [e] $MnBr_2$(dimethoxyethane). [f] Liquid at room temperature. [g] After 10 h reflux in dimethoxyethane. [h] After sublimation and recrystallizing twice.

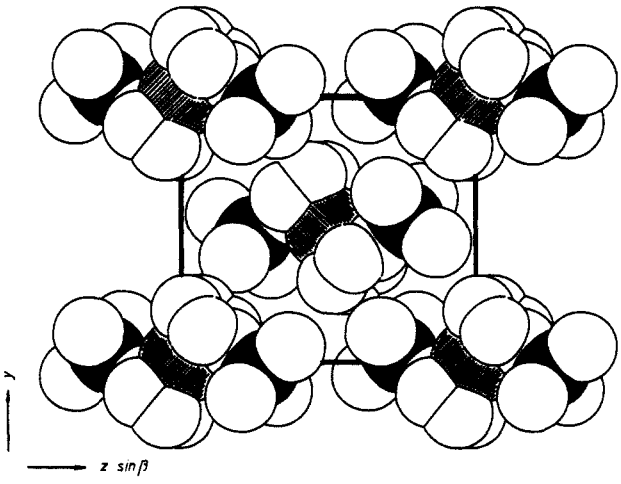

Figure 11. Crystal packing of $(Me_3SiCp)_2Mn$ in projection down the *a*-axis. For better visualization radii slightly smaller than in Figure 7b were used and H atoms were omitted: black, Si; hatched, Mn.

another origin must exist for $^6A_{1g}$-$(Me_3SiCp)_2Mn$: the antibonding character of only the symmetric e_{1g}* orbital in Figure 8 is reduced on introducing a silyl group. Hence, according to Figure 10 (one ligand has been omitted) and the qualitative carbon p_z electron densities given there the shortest bond should be Mn–C1 as found experimentally.

A second interesting structural feature of $(Me_3SiCp)_2Mn$ is the fact that there are no intermolecular bonding contacts which could be expected from the structure of Cp_2Mn.[16] Especially, the Cp slippage mentioned above is far from resembling the bridging η^3,η^2-Cp found by Weiss.[16] The packing of $(Me_3SiCp)_2Mn$ in the crystal is shown in Figure 11. It is determined largely by the arrangement of the silyl groups which, together with their trans-orientation in the molecule, reduces intermolecular interactions to a minimum. This is in accord with the low melting point.

The unique η^3,η^2-bridging cyclopentadienide in Cp_2Mn seems to be present in toluene solutions as well. The variable temperature ^1H results are best explained by the following equilibria. The

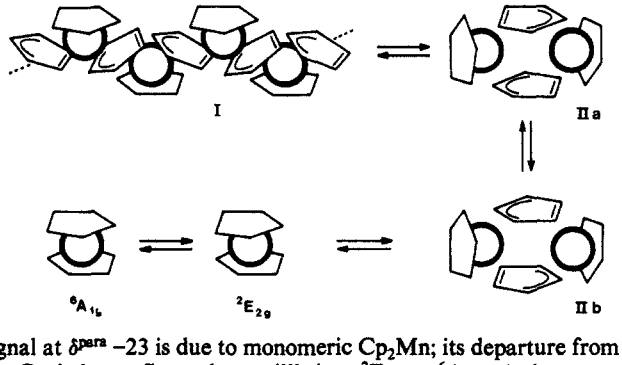

signal at δ^{para} −23 is due to monomeric Cp_2Mn; its departure from the Curie law reflects the equilibrium $^2E_{2g} \rightleftarrows {}^6A_{1g}$. At low temperature bridged species are formed on the expense of monomeric Cp_2Mn. At present we cannot distinguish between oligomeric and dimeric molecules I and II because both should give one signal for η^5-Cp and one for the η^3,η^2-Cp. The latter is a time-averaged signal of the two hapto parts which fluctuate as shown for IIa $\rightleftarrows$ IIb. It may be expected that this process is fast, and hence we are unable to see separate signals down to 180 K. Polymeric solid Cp_2Mn is antiferromagnetic;[2] we find a corresponding temperature behavior of the ^1H signals attributed to I and/or for II.

Conclusions

Modified manganocenes are now available in quantities useful for further reactions. The modification severely influences the spin state. The low-spin isomer is stabilized step-by-step on introducing donor substituents in the cyclopentadienide. Inversely, acceptor substituents stabilize the high-spin isomer. At present the minimum effort for the extremes is four methyls per Cp for low-spin and one silyl per Cp for high-spin species. Intermediate cases appear as low-spin–high-spin equilibria. For these equilibria again two extremes are realized by manganocene modification: in $(MeCp)_2Mn$ the life time of the spin isomers is long enough to be observed separately by NMR spectroscopy over a temperature range of 120 K while monomeric Cp_2Mn gives a mean signal only. Accordingly, NMR is shown to be the method of choice to fully characterize manganocenes.

A high-spin species is also stabilized by adding donor solvents to manganocenes. In these cases the coordination sphere of the metal is perturbed probably as a consequence of Cp lability. Such a lability is also met in inert solvents since Cp_2Mn tends to dimerize and/or oligomerize in solution via Cp bridges. Bridging in high-spin manganocenes can be prevented even in the solid state by bulky substituents like trimethylsilyl.

Experimetal Section

General Methods. The Schlenk technique was used to handle all metal organic compounds under dry oxygen-free argon. Solvents were dried over sodium or sodium–potassium alloy and distilled under argon from the desiccant before use. Moisture was removed from the glassware used in the final step of purification by heating under vacuum. Melting points were determined in a capillary sealed under argon. For elemental analysis liquid manganocenes were transferred into a small weighed glass tube which was closed at one end and equipped with a capillary at the other. The closed end was warmed, and the capillary was dipped quickly into the manganocene. On cooling, 5–15 mg of product were sucked in, and the capillary was sealed and broken immediately before the analytical procedure. The analyses were performed by the microanalytical laboratory of this institute.

The following compounds were prepared by literature procedures: CpNa and MeCpNa,[20,36] ethylcyclopentadiene,[37] isopropylcyclopentadiene,[38] *tert*-butylcyclopentadiene,[39] (trimethylsilyl)cyclopentadiene,[40] 1,2-dimethylcyclopentadiene,[41] tetramethylcyclopentadiene,[21] pentamethylcyclopentadiene,[42] ethyltetramethylcyclopentadiene,[43] $MnCl_2$,[17] and $MnBr_2$(DME).[44] Cyclopentadienes having more than two alkyl substituents were transformed to the lithium salts by addition of *n*-butyllithium in hexane to a solution of the cyclopentadienes in THF at −78 °C. The reaction mixture was brought to room temperature and used for further reactions. The other cyclopentadienes were converted to the potassium salts by reaction with potassium hydride in THF at 0 °C. After removal of excess KH the solutions were used directly for the syntheses of manganocenes. The content of cyclopentadienide was determined after hydrolysis by titration

with HCl; yields were between 96 and 99%.

Preparation of Manganocenes. Cp_2Mn (**1**) and $(MeCp)_2Mn$ (**2**) were synthesized similar to Wilkinson's procedures[2d,18] except that the sodium cyclopentadienides were prepared as mentioned above. For $(Me_5Cp)_2Mn$ (**9**) we followed Robbins et al.[5c]

Other Bis(mono- and disubstituted) Manganocenes. General Procedure. In a typical run 30 mmol of manganese(II) halide were suspended in 50 mL of THF. When $MnCl_2$ was used, $MnCl_2 \times 1.5$ THF[18] was formed in an exothermic reaction. The mixture was cooled to -20 °C, and 60 mmol of the dissolved cyclopentadienide were added with stirring and heated slowly to reflux. Within 6 h the solution became red. In some cases THF was replaced by higher boiling ethers like n-Bu_2O to make the reaction more efficient. After having removed the ether, the residue was extracted with 100 mL of pentane and washed with another four 20-mL portions of pentane. From the combined fractions the solvent was again removed, and the remainder was distilled at 8×10^{-2} Pa in an apparatus described in ref 20. Pure compounds were obtained when the distillation was kept slow (ca. 6 h) and when the film on the cooling finger was rejected twice at the beginning. Bis(ethyl-η^5-cyclopentadienyl)-manganese (**3**), bis(isopropyl-η^5-cyclopentadienyl)manganese (**4**), bis-(*tert*-butyl-η^5-cyclopentadienyl)manganese (**5**), bis(trimethylsilyl-η^5-cyclopentadienyl)manganese (**6**), and bis(1,2-dimethyl-η^5-cyclopentadienyl)manganese (**7**) were obtained in this way. Sublimation instead of distillation was used to isolate bis(tetramethyl-η^5-cyclopentadienyl)manganese (**8**) and bis(ethyltetramethyl-η^5-cyclopentadienyl)manganese (**10**). Preparative and analytical details are collected in Table VI.

NMR Measurements. When possible, the manganocene was freshly distilled into a 10-mm NMR tube equipped with a ground-glass joint; solvent and internal standard were added in case, and the sample was closed with a stopper. All spectra were recorded with a Bruker CXP 200 spectrometer with B VT 1000 temperature controller. Details such as instrumental parameters and temperature measurements were similar to those reported earlier.[34,45] Experimental shifts were measured relative to signals of the solvent or an internal standard and calculated relative to corresponding signals of isostructural ferrocenes to yield paramagnetic shifts, δ_T^{para} at a given temperature T with negative sign to low field. Details are given in the Supplementary Material. The errors were governed similarly by the line width Δ^{expt} and the above mentioned anisotropy effects: $\Delta^{expt} < 1$ kHz: δ better than ±0.5%; $\Delta^{expt} > 1$ kHz: δ ±1%. The temperature stability was better than ±0.3 K.

X-ray Structure Determination. A suitable single crystal was grown from a pentane solution at -78 °C after careful distillation of **6**. It was sealed under argon at dry ice temperature into a glass capillary and mounted on a four-circle diffractometer (Syntex $P2_1$). The monoclinic symmetry was checked by axial photographs and Delaunay reductions of the unit cell (TRACER). Exact cell dimensions were obtained by a least-squares fit of the parameters of the orientation matrix to the setting angles of 15 high angle reflections centered on the diffractometer. The crystal data as well as numerical details of the intensity data collection and structure refinement are given in Table III. One form of data was measured by a multispeed moving-crystal stationary-counter technique where the peak height at the calculated peak position served to determine the final scan speed. After Lp corrections a semiempirical absorption correction was applied because of the highly irregular crystal shape. This was based on scans at 10° intervals around the diffraction vectors of seven selected reflections near $\chi = 90°$ which served to determine the transmission curves (Syntex XTL). Since a reasonable density indicated $Z = 2$, the Mn atom was placed at the origin. (Due to the exceeding air and moisture sensitivity the experimental crystal density could not be determined). Subsequent Fourier and difference Fourier syntheses yielded the remainder of the molecule. After anisotropic refinement of the non-H atoms all hydrogens could be found in a difference synthesis. They were kept constant in further refinement cycles with the exception of those at the Cp ring which were refined isotropically. The function minimized in the refinement was $\Sigma w(|F_o| - |F_c|)^2$ with $w = k/\sigma^2(F_o)$ (SHELX 76). A final difference map was essentially featureless with the maxima in the vicinity of the methyl groups. Corrections for $\Delta f'$ and $\Delta f''$ were applied to all atoms. A detailed description of the data collection and refinement procedures is given elsewhere.[46] In this reference also the sources of the scattering factors are given.

Acknowledgment. We thank Professor P. Hofmann for helpful discussion. We are also grateful to the Fonds der Chemischen Industrie, Frankfurt for financial support.

Registry No. **1**, 73138-26-8; **2**, 32985-17-4; **3**, 101923-26-6; **4**, 85594-02-1; **5**, 101932-72-3; **6**, 101932-73-4; **7**, 101932-74-5; **8**, 101932-75-6; **9**, 67506-86-9; **10**, 101932-76-7.

Supplementary Material Available: Experimental NMR shifts, reference shifts of analogous ferrocenes, variable temperature NMR data for $(MeCp)_2Mn$, evaluation of $\Delta H°$ and $\Delta S°$, calculation of dipolar and contact shifts of the low-spin manganocenes, and additional crystal structure data tables of anisotropic temperature factors as well as observed and calculated structure factor amplitudes (11 pages). Ordering information is given on any current masthead page.

(36) Köhler, F. H. *J. Organomet. Chem.* **1976**, *110*, 235-246.
(37) Riemschneider, R.; Reichelt, E.; Grabitz, E. B. *Monatsh. Chem.* **1960**, *91*, 812-823.
(38) Köhler, F. H. *J. Organomet. Chem.* **1976**, *121*, C61-62.
(39) Riemschneider, R.; Reisch, A.; Horak, H. *Monatsh. Chem.* **1960**, *91*, 805-811.
(40) Davison, A.; Rakita, P. E. *Inorg. Chem.* **1970**, *9*, 289-294.
(41) Skattebøl, L. *J. Org. Chem.* **1964**, *29*, 2951-2956.
(42) Kohl, F. X.; Jutzi, P. *J. Organomet. Chem.* **1983**, *243*, 119-121.
(43) Feitler, D.; Whitesides, G. M. *Inorg. Chem.* **1976**, *15*, 466-468.
(44) King, R. B. *Metal Organic Syntheses*; Academic Press: New York, and London, 1965; Vol. I, pp 67-69.
(45) Köhler, F. H.; Hofmann, P.; Prössdorf, W. *J. Am. Chem. Soc.* **1981**, *103*, 6359-6367.
(46) Schmidbaur, H.; Herr, R.; Müller, G.; Riede, J. *Organomet.* **1985**, *4*, 1208-1213.

Fourier-Transform Infrared Linear Dichroism: Stretched Polyethylene as a Solvent in IR Spectroscopy

Juliusz G. Radziszewski and Josef Michl*

Contribution from the Department of Chemistry, University of Utah, Salt Lake City, Utah 84112. *Received October 18, 1985*

Abstract: The infrared linear dichroism of several dozen symmetrical organic molecules of low polarity has been measured on their solid solutions in stretched polyethylene and stretched perdeuterated polyethylene. Both saturated and unsaturated molecules, ranging in size from triatomics to tetracyclic aromatics, have been used. The orientation factors are dictated primarily by molecular shape, making these simple measurements useful for the determination of absolute polarizations of infrared as well as UV-visible transitions. The potential usefulness of the method for studies of molecular geometry and conformation is emphasized and illustrated on the simple case of aniline.

Among the characteristics of a transition in optical spectroscopy, the most fundamental ones are the energy (light frequency), intensity, and polarization, i.e., transition moment direction in the molecular framework. Whereas the first two have seen much use

0002-7863/86/1508-3289$01.50/0 © 1986 American Chemical Society